

Ruf, in Ref. 12, p. 610.

¹⁴Y. F. Bydin and A. M. Bukhteev, *Zh. Tech. Fiz.* **30**, 546 (1960) [*Sov. Phys. Tech. Phys.* **5**, 512 (1960)].

¹⁵B. I. Kikiani, G. N. Ogurtsov, N. V. Federenko, and I. P. Flaks, *Zh. Eksperim. i Teor. Fiz.* **49**, 379 (1965) [*Sov. Phys. JETP* **22**, 264 (1966)].

¹⁶R. E. Weber and L. F. Cordes, *Rev. Sci. Instr.* **37**, 112 (1966).

¹⁷J. C. King and J. R. Zacharias, *Advan. Electron. Electron Phys.* **8**, (1956).

¹⁸J. F. Cuderman, *Rev. Sci. Instr.* **42**, 1094 (1971).

¹⁹W. Wheeler, Research and Development Group, Vacuum Products Division, Varian and Associates, private communication.

vate communication.

²⁰J. Perel and H. Daley, in Ref. 12, p. 603.

²¹L. D. Landau, *Phys. Sowjetunion* **2**, 46 (1932).

²²C. Zener, *Proc. Roy. Soc. (London)* **A137**, 696 (1932).

²³E. C. G. Stueckelberg, *Helv. Phys. Acta* **5**, 370 (1932).

²⁴A. Russek, *Phys. Rev.* **132**, 246 (1963).

²⁵M. H. Mittleman and L. Wilets, *Phys. Rev.* **154**, 12 (1967).

²⁶O. B. Firsov, *Zh. Eksperim. i Teor. Fiz.* **36**, 1517 (1959) [*Sov. Phys. JETP* **36**, 1076 (1959)].

²⁷H. Fleischmann and R. Dehmel, in Ref. 12, Vol. II, p. 1146.

Formation of Fast Excited H Atoms. I. Charge-Transfer Neutralization of H⁺ in He and Ar[†]

J. C. Ford and E. W. Thomas*

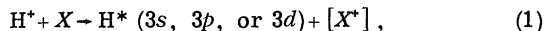
School of Physics, Georgia Institute of Technology, Atlanta, Georgia 30332

(Received 17 September 1971)

A study has been made of the charge-transfer processes whereby neutral atoms of hydrogen are formed in the $3s$, $3p$, and $3d$ states as a result of the impact of protons on targets of helium and argon. Impact energies range from 75 to 400 keV. The experimental procedures involve the quantitative measurement of the Balmer- α radiation emitted by the spontaneous decay of atoms in these three states. The contributions of the three different states are separated by a time-of-flight technique that utilizes the different lifetimes of these states. The cross sections decrease rapidly with increasing energy and are greatest for the state of lowest angular-momentum quantum number. For a helium target, comparisons are made with a Born-approximation prediction; there is a marked discrepancy between theory and experiment for the $3p$ level but good agreement for the $3s$ and $3d$ levels.

I. INTRODUCTION

The objective of the present study is the measurement of cross sections for formation of fast excited hydrogen atoms in the $3s$, $3p$, and $3d$ states by the impact of protons on helium and argon targets. The reaction may be described by



where X is either helium or argon. The square bracket in Eq. (1) indicates that there is no information on the post-collisional state of the target. The principal objective of the work was to test the theoretical predictions of charge-transfer cross sections. It has previously been argued¹ that formation of the $n=3$ levels by neutralization of H⁺ is a particularly useful case for making such tests.

II. EXPERIMENTAL TECHNIQUES

The formation of excited H atoms in the $3s$, $3p$, and $3d$ states can be detected by the quantitative measurement of Balmer- α photons emitted as excited atoms decay to the $n=2$ level. The Balmer- α (H_α) emission is, in fact, due to three transitions:

$3s \rightarrow 2p$, $3p \rightarrow 2s$, and $3d \rightarrow 2p$. These will emit photons of essentially the same wavelength and are therefore detected simultaneously. The separation of the three contributions is accomplished by a method which relies on the different lifetimes of the three states.

The experimental arrangement involves passing the beam through a target cell and measuring quantitatively the Balmer- α emission from the beam after it exits into an evacuated flight tube. Excited fast atoms, formed by neutralization in the target cell, decay in the observation region and produce an intensity whose spatial variation is related to the velocity of the atom and the lifetime of the excited state. The radiation may be described by an intensity function $I(X)$, where X is the distance from the termination of the gas cell. The function $I(X)$ is defined as the total number of Balmer- α photons radiated per second from a differential segment of beam dX about the point X . Since each state of excitation ($3s$, $3p$, and $3d$) has a distinctly different lifetime, the total intensity function $I(X)$ will be the sum of three spatially distinct and separable intensity functions, $I_{3s}(X)$, $I_{3p}(X)$, and $I_{3d}(X)$. The intensity $I_{3s}(X)$ is given by

$$I_{3l}(X) = A(3l - n = 2) n_{3l}^*(X), \quad (2)$$

here n_{3l}^* is the number of excited atoms per unit length of the beam at the point X , and $A(3l - n = 2)$ is the probability for spontaneous transition from the $3l$ state to the $n = 2$ level. It will be assumed that the population of the state is unaffected by cascade from higher levels; this assumption will be examined again later. It then follows that the X dependence of n_{3l} is governed solely by natural radiative decay; for particles of lifetime τ_{3l} and velocity v the spatial dependence comes from

$$\frac{dn_{3l}^*(X)}{dX} = \frac{-n_{3l}^*(X)}{v\tau_{3l}} \quad (3)$$

which has a solution

$$n_{3l}^*(X) = n_{3l}^*(0) e^{-X/v\tau_{3l}}. \quad (4)$$

The quantity $n_{3l}^*(0)$ is the number of excited atoms per unit length of the beam at the exit from the gas cell (i. e., at $X = 0$). This may readily be calculated² in terms of the length L of the gas cell, the density of the target ρ (molecules/cm³), the cross section for the charge-transfer process of interest Q_{3l} , and the flux of projectile ions traversing the target cell F (ions/sec);

$$n_{3l}^*(0) = FQ_{3l}\tau_{3l}\rho(1 - e^{-L/v\tau_{3l}}). \quad (5)$$

The development of this equation makes four assumptions; first, that there is no cascade population of the $3l$ state; second, that there is no collisional depopulation of the state; third, the density ρ remains uniform through the length of the target cell; fourth, that the flux of ions F is essentially the same at all points in the target cell. These assumptions will be examined again later.

Combining Eqs. (2), (4), and (5) the intensity function is given by

$$I_{3l}(X) = A(3l - n = 2)FQ_{3l}\tau_{3l}\rho[1 - e^{-L/v\tau_{3l}}]e^{-X/v\tau_{3l}}. \quad (6)$$

The lifetime τ_{3l} is identical to the inverse of the total probability for decay. It follows that $A(3l - n = 2)\tau_{3l}$ is the branching ratio for the decay $3l - n = 2$; the branching ratio is unity for the $3s - 3p$ and $3d - 2s$ transitions, and the ratio is 0.118 for the $3p - 2s$ transition.

In practice then, the intensity function $I(X)$ is a sum of three items like Eq. (4), one each for the $3s$, $3p$, and $3d$ states. The intensity $I(X)$ is experimentally measured as a function of X and fitted to the sum of the three exponential decays; from the values of $n_{3l}^*(0)$ so derived, the cross section Q_{3l} may be determined from Eq. (5).

The derivation of Eq. (6) proceeded on the assumption that the primary proton beam was not appreciably depleted by collisions in the gas cell and that no appreciable fraction of the excited atoms

underwent a collision before emission could take place. If either of these assumptions is not fulfilled, then Eq. (5) will be incorrect; in particular there will no longer be a linear dependence of intensity on pressure and beam flux. A necessary step in the experimental procedure is to confirm the linear relationships of intensity to both pressure and beam current for the operating conditions of the experiment; the established range of operating parameters is called "single-collision conditions." At sufficiently low values of both pressure and beam current that linear relationship must hold.

One of us (E. W. T.) has previously carried out an experiment¹ similar to the present work where observations were made of emission from the excited projectiles as they traversed the target. The intensity increased exponentially with distance of penetration through the gas in a manner similar to that described by Eq. (5). Again, in that case, the intensity of the Balmer emission was given by a sum of three terms which could be analyzed to give the three separate cross sections. A serious difficulty was that because of the considerable length of the gas target, collisional destruction of the long-lived $3s$ state took place before emission. That means the operating parameters did not constitute single-collision conditions and the analysis was thereby made very much more complicated. In the present work the target region is much shorter than for the early studies, and it proves possible to establish single-collision conditions. It follows that the present experiments involve a much simpler analysis than the previous work, and therefore the present data should be more accurate. The results and procedures of the previous experiments¹ are superseded by the present more satisfactory data.

III. CASCADE

The derivations of Sec. II are carried out on the assumption that the excited state is populated only by direct collisions [through the mechanism of Eq. (1)] and depopulated by spontaneous radiative decay. One can eliminate other collisional population mechanisms by establishing single-collision conditions. However, there is one population mechanism that cannot be eliminated in this manner, namely cascade transitions from higher levels.

Cascade has two important effects. First, it does of course complicate the relationship between the measured population and the cross section to be derived from it. Second, it introduces an additional term into the decay scheme characterized by the lifetime of the cascading state. This latter consideration is most important because a substantial cascade contribution will invalidate the whole basis of the analysis.

Consider cascade into the $3l$ level from a higher

state j . Adopting the same symbols as above, Eq. (3) must be modified to read,

$$\frac{dn_{3l}^*(X)}{dX} = \frac{-n_{3l}^*(X)}{v\tau_{3l}} + A(j \rightarrow 3l)\tau_j \frac{dn_j^*(X)}{dX}, \quad (7)$$

again $A(j \rightarrow 3l)$. τ_j represents the branching ratio for decays from the state j to the state $3l$. In order to solve (7) one needs to know n_j ; as a first approximation, we assume that cascade into j can be neglected, and therefore decay of that state is represented as in Eq. (4),

$$n_j^*(X) = n_j^*(0) e^{-X/v\tau_j}. \quad (8)$$

Substituting Eq. (8) into Eq. (7) one may arrive at

$$n_{3l}^*(X) = \left[n_{3l}^*(0) - n_j^*(0) A(j \rightarrow 3l) \left(\frac{\tau_i \tau_{3l}}{\tau_{3l} - \tau_j} \right) \right] e^{-X/v\tau_{3l}} + \left[n_j^*(0) A(j \rightarrow 3l) \left(\frac{\tau_j \tau_{3l}}{\tau_{3l} - \tau_j} \right) \right] e^{-X/v\tau_j}. \quad (9)$$

This is to be compared with Eq. (4) which is the equivalent expression with no cascade. It should be noted that the quantities $n_{3l}^*(0)$ and $n_j^*(0)$ do still represent the population of the $3l$ and j states at $X=0$; however their interpretation in terms of cross sections is not as simple as indicated by Eq. (5).

The first step in the analysis procedure was to make a least-squares fit of the three-term decay equation to the experimental data points; the decay equation was a sum of terms like Eq. (6) for each of the $3s$, $3p$, and $3d$ states. The fit of the decay equation to the data points was deemed to be satisfactory when the discrepancy between the fitted curve and each datum point did not exceed the statistical accuracy of that datum point. In cases where a satisfactory fit is obtained with a three-term decay equation one concludes that cascade is unimportant. One may have a situation where the deviation of the fitted curve from data points does exceed the statistical accuracy of the data; in this case one must conclude that the three-term decay equation does not adequately represent emission from the excited states and that cascade is significant. In principle one might attempt to introduce cascade terms like Eq. (9) and thereby determine cross sections for the $3s$, $3p$, and $3d$ states under circumstances where cascade is significant.

For the present work on charge transfer a satisfactory fit was obtained with the three exponentials characterizing the $3s$, $3p$, and $3d$ states; no cascade term was necessary. It is therefore concluded that, to within the accuracy of the experimental measurements the contribution of cascade transitions has negligible influence on the determination of cross sections for the $3s$, $3p$, and $3d$ states.

IV. APPARATUS

The apparatus for the experiment is shown schematically in Fig. 1. The source of incident protons was a 1-MeV Van de Graaf positive-ion accelerator with a beam analyzing and stabilizing system. The incident proton energy was determined to within ± 2 keV by deflection in a regulated magnetic field. The projectile beam was collimated by two 1.5-mm-diam knife-edged circular apertures separated by a distance of 17 cm. All other apertures are larger than these two collimators in order that they should not intercept any appreciable fraction of the projectiles. Following the collimator the beam was directed through the cell containing the target gas and then into an evacuated flight tube; in this latter section the optical observations are carried out and the beam current is monitored. The ion beam current through the target was typically 1 to 3 μ A.

The target cell was 14 cm long with channels at either end through which the beam entered and exited. At the exit aperture was an annular plate that picked up any current of particles scattered out of the beam path; current to that electrode represented the flux of projectiles that was intercepted by the exit orifice. At all times this flux was kept less than 0.01% of the projectile beam current. The target gas was passed through a cold trap to remove condensable materials and then leaked into the collision chamber. Impurity concentrations were stated by the gas suppliers to be less than 0.01%. The target-gas pressure was monitored continuously by a capacitance manometer; the calibration of the manometer had previously been checked against a McLeod gauge with proper attention to removing errors caused by cold-trap pumping and thermal transpiration. The temperature of the target-cell walls was also monitored continuously. Temperature and pressure were used in the ideal-gas equation to calculate target density. Continuous monitoring of temperature proved to be rather important since it rose by some 3 to 5 $^{\circ}$ C during a single experimental run. This heating was caused by the projectile beam intercepted on the collimators.

The current of primary ions was monitored on a deep Faraday cup situated at the end of the flight tube. Biases were provided to suppress secondary electrons ejected from the base of the Faraday cup. A large grounded plate isolated the electrostatic fields of the Faraday cup from the observation region.

The observation chamber was fitted with a plate glass window through which the beam line could be viewed. The photon detector, consisting of a lens assembly, interference filter, aperture and photomultiplier, was mounted on a specially constructed travelling platform. This platform could be posi-

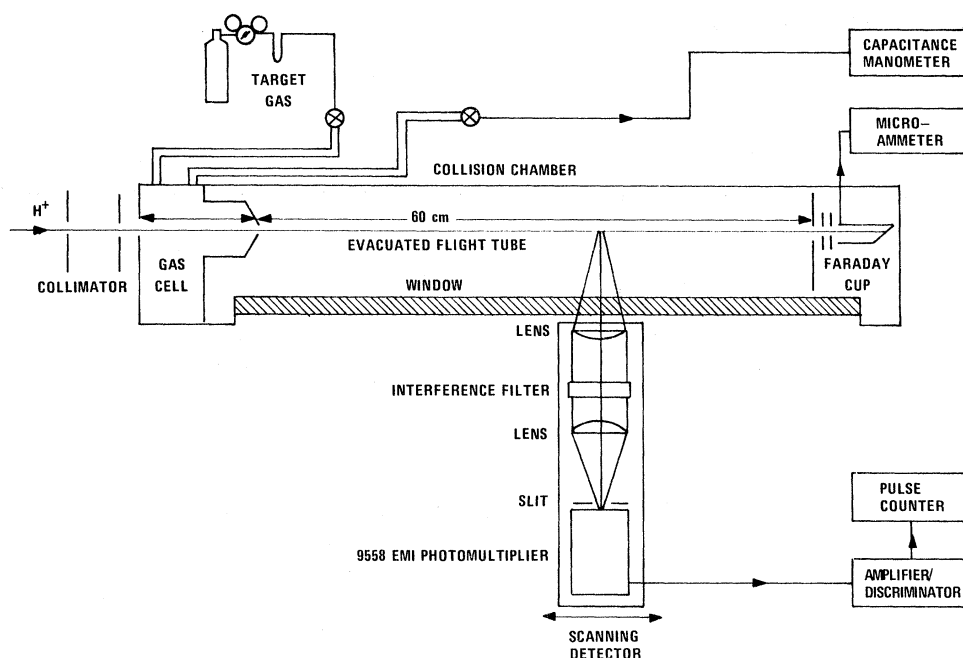


FIG. 1. Schematic diagram of the apparatus.

tioned automatically at different distances X from the target-cell exit; once aligned with the beam it would accurately maintain its orientation. Two plano-convex lenses focus an image of the beam onto the surface of a photomultiplier; the interference filter was placed between the two lenses. An aperture at the image plane permits only light from a 6-mm-long segment of the beam path to fall on the multiplier. The photomultiplier (EMI type 9558) was operated in a pulse counting mode; the tube was cooled to reduce the dark count. A survey was made of the point-to-point variations in sensitivity over the face of the tube, and its orientation was chosen such that the variation in sensitivity over the exposed portion was less than 2%.

The operating procedure was to record photon count, target pressure, and beam current for a series of positions at different distances X from the target-cell exit; the distance X extended to 65 cm from the target-cell exit. From these figures and the apparatus constants, was calculated $I(X)$, the intensity at each position X . The complete set of points was fitted by a sum of the three relevant decay equations [Eq. (4)]; the values of $n_{31}^*(0)$ were determined and hence the cross sections evaluated [from Eq. (5)].

The analysis of the raw data involved a number of small corrections. These included the dark current of the multiplier and small drifts of the instrumental zeros. A more important effect was a correction to take into account the flow of gas from the target cell into the flight region. This may

produce a contribution to the signal both from formation of excited H atoms by charge transfer and also by excitation of the gas itself. The gas in the flight tube was taken into account as follows. First the full measurement of $I(X)$ was made as described above; the pressure rise in the flight tube due to entry of gas from the target was recorded. Then the cell was evacuated and target gas introduced into the flight tube to a pressure equal to that used during the previous stage; again the intensity function is recorded. The differences between the two intensity functions represents the true contribution from charge transfer on the target gas; this set of figures was used for determination of cross section.

V. CALIBRATION

An important feature of the present work is that the detection sensitivity was determined by direct calibration, and the cross sections thereby placed on absolute basis. This requires two distinct steps; first the measurement of how detection sensitivity varies with projectile velocity as a result of Doppler effects and secondly the absolute calibration itself.

As a result of the excited atom's high velocity the emission exhibits substantial wavelength shift through the Doppler effect. The optical system accepts light emitted into a 12° cone centered at 90° to the beam axis. Consequently, the emission incident on the filter exhibits a Doppler broadening which ranges from 34 \AA at 75 keV to 80 \AA at 400 keV. Since the interference filter selects only a narrow bandwidth of radiation, the effective sensi-

tivity of the detector varies with the input energy of the incident protons. It is emphasized that this dependence influences only the absolute value of $I(X)$; it does not influence the relative values of $n_{3s}^*(0)$, $n_{3p}^*(0)$, and $n_{3d}^*(0)$ deduced from the fitting of exponentials to the decay curve. The following technique was devised to correct for the variation in sensitivity. The optical aperture of the detector arrangement was divided into a series of elements. The actual wavelength of light incident on each element was determined from the formula for Doppler shift; with a knowledge of filter transmission as a function of wavelength it was then possible to determine the relative contribution of each element to the over-all sensitivity. The contributions from these elements were then summed over the whole aperture. Carrying out this procedure for each projectile velocity, one arrives at a relative variation of sensitivity with projectile velocity. The result of such a procedure has been shown in our previous work (Fig. 2 of Ref. 1).

The second step was the absolute calibration of detector sensitivity against a standard source at the wavelength of 6563 Å; this corresponds to a calibration for a vanishingly low particle velocity when Doppler shift can be neglected. As a basis for calibration, a standard tungsten-strip filament lamp was utilized. The output of this lamp at a given filament temperature is known in terms of the emission of a blackbody and the emissivity of tungsten.³ The standard source was placed at the optical position normally occupied by the projectile beam; the response of the equipment was determined and the temperature of the filament measured by an optical pyrometer. Account was taken of the fact that the standard produces a continuum rather than a discrete line emission.

A complicating feature of the analysis is that the observation region is not in fact a point source; as a result the light from certain parts of the observation region is not normal to the interference filter. This causes the transmission of the filter to be slightly dependent on the emitting atom's precise position in the observation region. The standard source had dimensions that exceeded those of the observation region; consequently the filter transmission when observing collisionally induced emission is exactly the same as the transmission when the standard is observed. It follows that the observation region's finite dimension does not cause an error in the quantitative measurement of the emission.

The calibration provides a direct absolute measurement of cross section in terms of the emissive power of a blackbody and the emissivity of tungsten. This is in contrast to our previous study of the charge-transfer problem¹ where absolute values were assigned by normalization to an earlier mea-

surement of a cross section for excitation of a target gas. Being more direct, the present data are to be preferred.

VI. PRESSURE GRADIENTS

An attempt was made to take into account the inevitable pressure gradients at the exit and entrance to the cell. As a result of such gradients the target density ρ is not completely uniform and the cell length L is not equal to the distance between the exit and entrance apertures.

A calculation was made of the pressure gradient along the entire length of the cell with the assumption that molecular-flow conditions were applicable. Outside the exit aperture, the calculated pressure profile was confirmed experimentally by placing helium in the cell and observing with the optical system the intensity profile of a helium spectral line in the flight tube. Helium gas will be collisionally excited by the projectiles and the intensity distribution should indicate the relative shape of the gas density profile. On the basis of these calculations and observations a correction was evaluated to take into account the gradients. The correction was up to 30% for the $3p$ level at low velocities; it is large for the $3p$ level because the decay length for this state is of approximately the same magnitude as the extent of the density gradient. In the case of longer-lived $3s$ and $3d$ levels this correction was less than 10%.

VII. EFFECTS OF POLARIZATION

Emission from the $3p$ and $3d$ states may be polarized; such polarization is governed by the different cross sections for populating the magnetic substates, and it will cause anisotropy of the emission. The influence of polarization was ignored in the present work. It has been previously shown¹ that neglect of polarization will cause a maximum uncertainty of +9 to -14% in the cross section for the $3p$ state and +11 to -16% for the $3d$ state. These limitations are included in the estimated uncertainties of the data.

VIII. EXPERIMENTAL UNCERTAINTY

Random errors in the data arose from the statistical limitations of the photon detection as well as small drifts in the instrumental sensitivities and zeros. The resulting error in $I(X)$ could be assessed by repetitive measurements over an extended period of time. Such errors in $I(X)$ were typically of the order $\pm 1\%$. The errors in the derived cross sections are not equal to this quantity; random errors in $I(X)$ will cause a large influence on the short-lived $3p$ and $3d$ components but smaller errors in the $3s$ contribution. A model calculation was carried out in which the values of $I(X)$ at different X were varied through a range appropriate to the

random errors of the measurements. Each target involved somewhat different results due to the different cross sections; as an example, for argon it was concluded that the random error in the $3s$ cross section did not exceed $\pm 7\%$, the error in $3d$ and $3p$ did not exceed $\pm 20\%$.

The possible random errors in the $3p$ - and $3d$ -state cross sections do have the appearance of being unreasonably large. However it must be noted that the maximum contribution to the signal for the $3d$ state is of the order 1 to 2% of the total and that for the $3p$ state is 10% or less; that is caused by a combination of small cross sections, short decay lengths, and, for the $3p$ state, an adverse branching ratio. It follows that even if the total random error during an experimental run is kept to less than 1% then there will still be large random error in the derived cross sections for the $3p$ and $3d$ states.

It is necessary to consider the influence of small uncertainties in the excited-state lifetime τ , and the particle velocity v . The lifetimes were taken from theoretical calculations⁴; these are believed to be accurate to within 1%. The particle energy is determined to within ± 2 keV with the momentum selector of the accelerator. One may calculate that at distances X which greatly exceed the decay length (product of v and τ) a small error in v or τ will cause a large percentage change in intensity. However, at such large distances the intensity is very small and data points in this region are relatively unimportant in establishing cross section. A model calculation is the most satisfactory manner for a proper quantitative estimate of the influence of errors in the values of τ and v . One may take an intensity function $I(X)$ and go through the procedure of fitting the sum of three exponential decay terms to determine cross sections. One then repeats the fitting procedure but with velocity of lifetime changed by a fixed amount. The difference between cross sections determined using the two different sets of lifetimes, or velocities, is a direct indication of the uncertainty in cross-section values that may be ascribed to an error in the assumed value of lifetime or velocity. We did not use an actual data set for this test; rather we employed a synthesized decay curve generated by taking expressions like Eq. (6) for each of the $3s$, $3p$, and $3d$ states. The synthesized decay curve was generated using physically realistic cross sections. First, one carries out the curve-fitting procedure using the same lifetimes and velocities that were utilized to generate the synthesized curve; naturally one recovers the same cross sections that were used in the generation of that curve. The procedure is then repeated with a changed value of velocity and lifetime; a further cross-section value is deduced. Typically a 1% change in velocity of life-

time produced changes in the $3s$, $3p$, and $3d$ cross sections of, respectively, 0.5, 0.5, and 1.5%.

These errors are negligible compared with the random errors associated with the statistical limitations of the photon detection.

The systematic errors are incurred primarily through the procedures for determining the various instrumental calibration factors; the important quantities here are the beam current, the target density, and the detection sensitivity. The accuracy of the beam-current measurement was established by checking the calibration of the current-measurement electrometer; this test was carried out with a current source composed of standard resistance and a standard voltage. The errors in this instrumental calibration were found to be less than 2.5%. The calibration of the pressure-measurement device was checked by comparing it to a McCleod gauge using hydrogen as the test gas; proper precautions were taken to prevent cold-trap pumping and thermal transpiration effects.⁵ The McCleod gauge and the capacitance manometer agreed to within 1%; allowing for a possible error in the McCleod gauge reading of up to 5%, we establish the maximum uncertainty in pressure measurement to be 6%. The calibration of detection sensitivity employed a tungsten-strip filament lamp as a standard of emission; the emissive power of such a lamp is known accurately as a function of filament temperature.³ The major source of error in the use of this standard lamp arose from the establishment of filament temperature by measurements with an optical pyrometer. The uncertainty in temperature is the sum of two quantities. First, there is the limit of accuracy associated with the pyrometer calibration; this was taken from the manufacturers specifications. The second is the reproducibility with which the operator can set the pyrometer; this quantity is indicated by the spread of values in the repetitive measurement of a constant temperature source. The possible error in determination of temperature can then be used to estimate the corresponding uncertainty in intensity; this amounts to 15% for the present work. We choose to estimate the limit of accuracy of the cross-section values by taking the root of the sum of the squares of the possible errors in current, pressure, and intensity measurement that are listed above; that estimate is 16.5%.

There is also a possible error in the velocity-dependent correction for the sensitivity changes associated with Doppler shift. Any such error might cause the energy dependence of cross sections to be incorrect. The Doppler-shift corrections amount to 30% at the highest energies and are negligible at low energies (75 keV). We estimate that the whole procedure for establishing this correction is accurate to better than 10%. It follows that errors

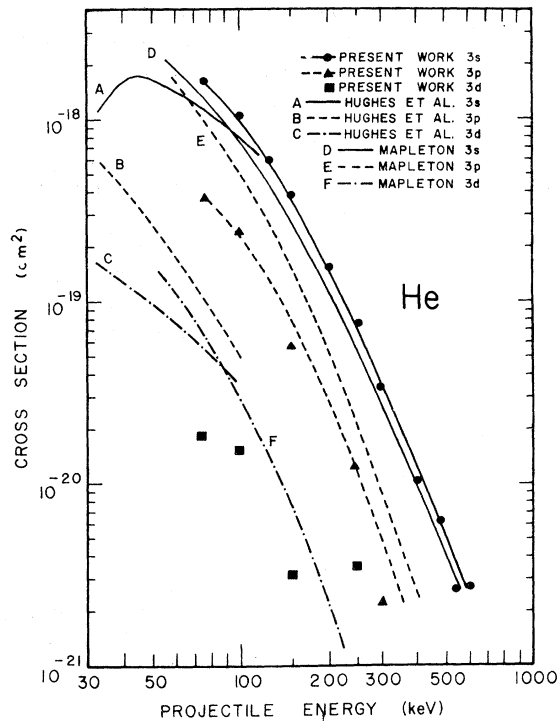


FIG. 2. Cross sections for the formation of H(3s), H(3p), and H(3d) atoms by charge transfer in helium. Present measurements are shown along with those made by Hughes *et al.* (Ref. 6). Also presented are the predictions of the Born approximation calculated by Mapleton (Ref. 8).

in the decay dependence of cross-section values should not exceed 3%.

In summary, the systematic error in the absolute values of the whole set of cross-section values should not exceed 16.5%. Energy-dependent systematic errors that cause inaccuracy of the functional relation between cross section and energy will be less than 3%; this is rather small compared with other uncertainties. The random errors in the 3s data points should be less than $\pm 10\%$ for helium and $\pm 7\%$ for argon. Random uncertainties in the 3p and 3d data are very much higher due to their small contribution to the total signal and to the neglect of polarization. It is estimated that the error bars for helium range from -64 to $+59\%$ for the 3p state and -84 to $+59\%$ for the 3d state. In argon the signals are higher and the corresponding limits for the 3p level are -34 to $+29\%$ and the 3d level -31 to $+26\%$.

IX. CHARGE TRANSFER IN HELIUM

In Fig. 2 are shown the cross-section measurements for charge transfer in helium. Also shown on this figure are an independent set of measurements at lower velocities by Hughes *et al.*⁶ The two sets of data for 3s and 3d levels agree within

the limits of experimental accuracy. There is, however, a considerable discrepancy in the case of the 3p level. A possible explanation for part of this discrepancy may be found in the neglect of corrections [by Hughes *et al.*] for pressure gradients at the gas-cell exit aperture. It is also to be noted that the 3p-state measurement must be the least accurate of the set because of its short lifetimes; the resulting short decay length requires that the measurement be based primarily on readings at only one or two values of X . There are also measurements of the 3s cross section at lower energies carried out by Andreev *et al.*⁷ These are also in complete agreement with the work of Hughes *et al.*⁶ The good agreement between these three completely independent measurements lends confidence to the accuracy of the present work.

There is also previous work by one of us (E. W. T.) on this same problem.¹ These early data are less accurate than the present work and did not involve an absolute calibration. It follows that the earlier measurements on charge transfer¹ are superseded by the present data. In fact the earlier data are consistent with the present work within the combined limits of accuracy of both experiments.

Also shown in Fig. 2 are theoretical predictions of these cross sections by Mapleton⁸ in the Born

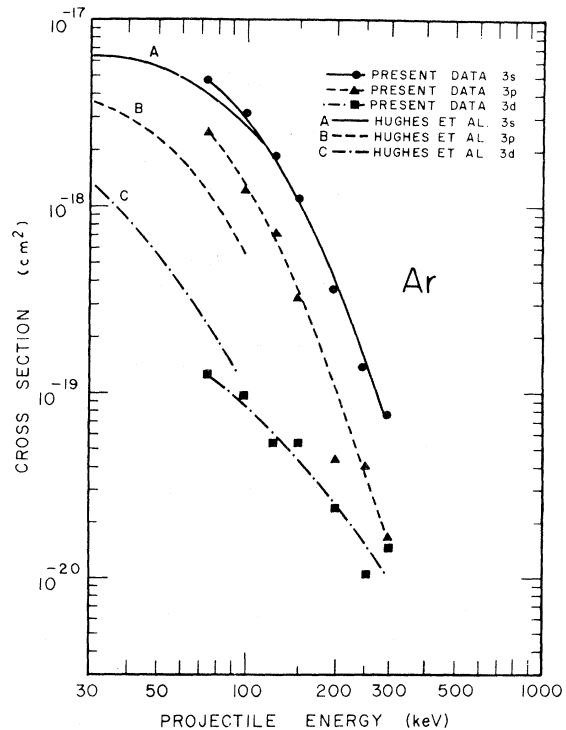


FIG. 3. Cross sections for the formation of H(3s), H(3p), and H(3d) atoms by charge transfer in argon. Present measurements are shown along with those by Hughes *et al.* (Ref. 6).

approximation. It would appear that theory and experiment are quite consistent for the 3s and 3d levels. For the 3p state, however, the theory consistently lies above the experiment by a factor of 2 or more; moreover, there is a significant difference between the energy dependence of theory and experiment.

X. CHARGE TRANSFER IN ARGON

In Fig. 3 are shown the cross sections for argon. Again a comparison may be made with work by Hughes *et al.*⁶; the 3s and 3d cross sections are consistent but again the 3p cross section of the present work lies above that measured by Hughes *et al.*

[†]Supported in part by the Controlled Thermonuclear Research Program of the U. S. Atomic Energy Commission.

*Temporary address: FOM Institute for Atomic and Molecular Physics, Kruislaan 407, Amsterdam, The Netherlands.

¹J. L. Edwards and E. W. Thomas, *Phys. Rev.* **2**, 2346 (1970).

²Reference 1, Eq. (5).

³J. D. De Vos, *Physica* **20**, 690 (1954).

⁴W. L. Weise, M. W. Smith, and B. M. Glennon, *Atomic Transition Probabilities, Hydrogen Through Neon*,

For argon it is noted that the fraction of the $n = 3$ level population formed in the 3p state is somewhat higher than in the case of helium.

XI. CONCLUSION

Charge transfer into the 3s and 3d states on a helium target is in good agreement with the theoretical predictions by a Born approximation. The theoretical predictions for the 3p state, however, do exceed the measured values by a significant amount. It appears that the Born approximation is a satisfactory procedure for the calculation of these cross sections in the energy range of the present experiments.

National Standard Reference Data Series—National Bureau of Standards 4 (U. S. GPO, Washington, D. C., 1966), Vol. I.

⁵P. H. Carr, *Vacuum* **14**, 37 (1964).

⁶R. H. Hughes, C. A. Stigers, B. M. Doughty, and E. D. Stokes, *Phys. Rev. A* **1**, 1424 (1970).

⁷E. P. Andreev, V. A. Ankudinov, and S. V. Bobashev, *Fifth International Conference on the Physics of Electronic and Atomic Collisions, Leningrad, 1967* (Nauka, Leningrad, 1967), p. 307.

⁸R. A. Mapleton, *Phys. Rev.* **122**, 528 (1961).

Formation of Fast Excited H Atoms. II. Charge-Transfer Neutralization of H⁺ on Molecular Gases*

J. C. Ford and E. W. Thomas[†]

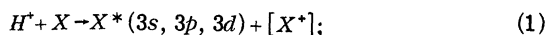
School of Physics, Georgia Institute of Technology, Atlanta, Georgia 30332

(Received 17 September 1971)

An experimental study is made of the cross sections for forming fast hydrogen atoms in the 3s, 3p, and 3d states by charge-transfer neutralizations of H⁺ as it traverses molecular targets. The formation of excited hydrogen is detected by a quantitative measurement of collisionally induced Balmer- α emission; the contributions from the 3s, 3p, and 3d levels are separated by a method that utilizes the different lifetime of the excited states. Proton-impact energies range from 75 to 700 keV; targets include H₂, N₂, NO, O₂, CO, CO₂, CH₄, C₂H₄, C₂H₆, and C₃H₈. Cross sections decrease rapidly with impact energy; the 3s cross section was always largest followed by the 3p and 3d. There was no convincing evidence for a general additive rule whereby cross sections could be assigned to the individual constituent atoms of the molecule and then used to predict cross sections for complex molecules.

I. INTRODUCTION

A study has been made of the cross sections for formation of fast excited hydrogen atoms in the 3s, 3p, and 3d states as a result of charge-transfer neutralization when protons traverse a molecular gas. The reaction equation may be written



here the square brackets indicate that the experi-

ments give no information on the state of excitation, ionization, or molecular association in which the post-collision target state is formed.

For the case of H₂ and N₂ targets a full study was made of the three cross sections over a wide range of energies. For targets of NO, O₂, CO, CO₂, C₂H₂, C₂H₄, C₂H₆, and C₃H₈ the data were restricted to measurements of the 3s state at three different impact energies only.

The techniques used in these measurements are